

## Manganian kinoshitalite in Mn-rich marble and skarn from Virginia

ROBERT J. TRACY<sup>1,\*</sup> AND JAMES S. BEARD<sup>2</sup>

<sup>1</sup>Department of Geological Sciences, Virginia Tech, Blacksburg, Virginia 24061-0420, U.S.A.

<sup>2</sup>Virginia Museum of Natural History, 1001 Douglas Avenue, Martinsville, Virginia 24112, U.S.A.

### ABSTRACT

A new locality for the Ba-rich trioctahedral mica, kinoshitalite [Ba(Mg,Mn,Fe,Al)<sub>3</sub>Si<sub>1.9-2</sub>Al<sub>2.2</sub>O<sub>10</sub>(OH,F)<sub>2</sub>], has been found in a metamorphosed manganian marble from Pittsylvania County, Virginia. Metamorphic grade is middle amphibolite facies, with documented *P* and *T* of 400 MPa and 575 °C. The locality is along strike not far from the well known Bald Knob, North Carolina, Mn-mineral locality, and appears to represent a silica-poorer analog of Bald Knob. The kinoshitalite occurs in a single layered hand sample containing both skarn and marble layers, and it shows significant compositional contrasts between the two lithologies. Kinoshitalite is scarce and fine-grained in manganian marble and coexists with kutnahorite, manganian calcite, fluorian alleghanyite, fluorian sonolite, aluminous jacobsonite, and alabandite. Kinoshitalite is both more abundant and coarser-grained in skarn where it coexists with kutnahorite, tephroite, fluorian manganhumite, spessartine, jacobsonite, and manganian magnetite. A-sites in kinoshitalite in skarn are about 3/4 occupied by Ba (with the remainder mostly K), whereas in marble, Ba occupancy of A-sites exceeds 90% and most of the remainder is Ca.  $X_{Mg}$  in octahedral sites is >0.6 and is higher in marble than in skarn, whereas  $X_{Mn}$  is significant (>0.2) and is higher in skarn than in marble. The <sup>VI</sup>Al is significantly higher in skarn kinoshitalite, as is total Tschermak content. The total Tschermak content of these barian micas (<sup>VI</sup>Al + Ti + Fe<sup>3+</sup>) is typical of all previously reported kinoshitalites and is significantly lower than that of clintonite and biotite. The  $X_F$  of kinoshitalite in marble is significantly higher than that in skarn.

The petrogenesis of kinoshitalite at the Hutter Mine locality is unclear due to the lack of context for the single mine-dump sample in which the mineral was found and the absence of textural evidence for reactions. However, the two likeliest source minerals for Ba that have been found in the deposit are barite and BaCa(CO<sub>3</sub>)<sub>2</sub> (probably barytocalcite). One hypothetical reaction to produce kinoshitalite involves decarbonation, in which BaCa(CO<sub>3</sub>)<sub>2</sub>, rhodochrosite, Mn-garnet, and aqueous fluid react to form kinoshitalite, tephroite (or an Mn-humite), calcite, and CO<sub>2</sub>. A second potential reaction to form kinoshitalite involves barite, Mn-garnet, tephroite, and aqueous fluid as reactants, and kinoshitalite, alabandite, jacobsonite, SiO<sub>2</sub>, and O<sub>2</sub> as products.

### INTRODUCTION

Kinoshitalite, Ba-rich phlogopite [ideally BaMg<sub>2</sub>Al<sub>2</sub>Si<sub>2</sub>O<sub>10</sub>(OH)<sub>2</sub>] is a member of the brittle-mica group of sheet silicates (Guggenheim 1984). It was first reported by Yoshii et al. (1973) from the Noda-Tamagawa mine, Japan, an amphibolite- to granulite-facies metamorphosed Mn deposit (Watanabe et al. 1970). Ba-rich micas have been reported from various geologic settings: alkalic igneous rocks (e.g., Thompson 1977; Wendlandt 1977; Mansker et al. 1979; Gaspar and Wyllie 1982; Edgar 1992; Zhang et al. 1993), metasomatic rocks (e.g., Pan and Fleet 1991; Harlow 1995), marbles or calc-silicates (e.g., Pattiarachi et al. 1967; Glassley 1975; Rice 1977; Bücher-Nurminen 1982; Solie and Su 1987; Bol et al. 1989; Tracy 1991), and metamorphosed Mn-bearing ore deposits (e.g., Frondel and Ito 1967; Yoshii et al. 1973; Matsubara et al. 1976; Dasgupta et al. 1989; Tracy 1991; Chabu and Baulège 1992; Frimmel et al. 1995; Dunning and Cooper 1999; Gnos and Armbruster 2000).

There are three trioctahedral brittle micas for which natural representatives show substantial or total occupancy of the

interlayer site by Ba<sup>2+</sup>: (1) kinoshitalite, (2) anandite, which has S<sup>-2</sup> and is rich in Fe (Pattiarachi et al. 1967; Filut et al. 1985), and (3) ferrokinoshitalite, an Fe-rich analogue of kinoshitalite (Tracy 1991; Frimmel et al. 1995; Guggenheim and Frimmel 1999). The South African "Fe-kinoshitalite" (Frimmel et al. 1995) is surprisingly F rich for such an Fe-rich mineral, with virtually no Cl, whereas the occurrence at Sterling Hill, New Jersey (Tracy 1991) shows very high Cl (up to 80% of the hydroxyl site occupied by Cl). Most kinoshitalites are Mn-bearing to Mn-rich, and have been found exclusively in middle amphibolite- to granulite-facies metamorphosed Mn deposits (Gnos and Armbruster 2000), however, an Fe-bearing but Mn-poor kinoshitalite from Alaska was reported by Solie and Su (1987).

The kinoshitalite from the Hutter Mine deposit in Pittsylvania County, Virginia, occurs in manganian marble and associated skarn. The Hutter Mine, an important locality for Mn minerals (Beard et al. 2002), is about 80 km along strike from the well known Mn-mineral locality at Bald Knob, near Sparta, North Carolina (Simmons et al. 1981). Although similar to Bald Knob in many respects, including metamorphic grade

\* E-mail: rtracy@vt.edu

(Winter et al. 1981), the Hutter Mine locality appears to be a silica-poor analog, based on the contrasting presence of manganosite ( $\text{MnO}$ ) and absence of the pyroxenoids rhodonite and pyroxmangite (roughly  $\text{MnSiO}_3$ ) at Hutter, compared to Bald Knob. Manganosite stability in particular appears to be very sensitive to elevated silica activity (Beard and Tracy 2002).

Kinoshitalite has only been found in one large, layered marble-skarn rock sample from a mine dump at Hutter. In the marble layer, it is associated with kutnahorite, manganian calcite, fluorian alleghanyite, fluorian sonolite, aluminous jacobsonite, and alabandite, whereas in the skarn, it occurs with kutnahorite, tephroite, fluorian manganhumite, spessartine, aluminous jacobsonite, and manganian magnetite. Other Ba minerals found in the deposit, although not in the kinoshitalite-bearing sample, include barite and Ba-Ca carbonate (probably barytocalcite). These minerals may have played a role in the genesis of kinoshitalite during higher-grade metamorphism.

The crystal structure of kinoshitalite is thought to be  $1M$ , with hypothetical polytypes  $C2$ ,  $C\bar{1}$ , and twinned variants of both of these (Guggenheim 1984; Brigatti and Poppi 1993; Gnos and Armbruster 2000). We have not as yet performed X-ray studies on the Hutter Mine material, but focus in this paper on the significant chemical variations we have found that are correlated with lithologic differences in the host rock. In the paper we will explore the systematic compositional differences between kinoshitalites in the skarn and marble lithologies. These include higher Ba contents in the marble, coupled with substantial Ba-Ca mixing in the interlayer site (and with virtually no K). Kinoshitalite in skarn shows lower Ba contents, coupled with Ba-K interlayer-site mixing (with virtually no Ca). In addition, kinoshitalites in the marble are significantly richer in F whereas those in skarn are substantially more Mn-rich. These chemical contrasts will be discussed in light of a model for kinoshitalite formation at this locality.

## GEOLOGIC SETTING

The Hutter Mine is located near the town of Pittsville, in northern Pittsylvania County, Virginia (Fig. 1). The locality is within the Smith River Allochthon (SRA), a thrust-bounded sequence of metamorphosed Late Precambrian to Middle Cambrian sedimentary, volcanic, and volcanoclastic rocks associated with a poorly understood volcanic arc system of apparent non-North American affinity (Hibbard et al. 2003). The SRA consists of two stratigraphic units above the Bowens Creek Fault, the lower bounding thrust fault of the allochthon: the Bassett Formation (largely amphibolites, with subordinate calc-silicates and felsic gneisses) and the Fork Mountain Formation (dominantly pelitic schists and gneisses, with minor amphibolite). Metamorphism of the rocks in the SRA occurred at about 530 Ma (Lanzirotti and Hanson 1997; Tracy et al. 2001).

The Hutter Mine deposit lies within schist of the Fork Mountain Formation just to the southwest of the James River–Roanoke River manganese-iron-barite district (Beard et al. 2002). This linear belt of mineralization in metasedimentary and metavolcanic rocks of the Eastern Blue Ridge Province is associated with quartzitic layers in pelitic schists and particularly with thin layers or lenses of marble lying along schist-quartzite contacts near greenstone (metabasalt) layers (Watson

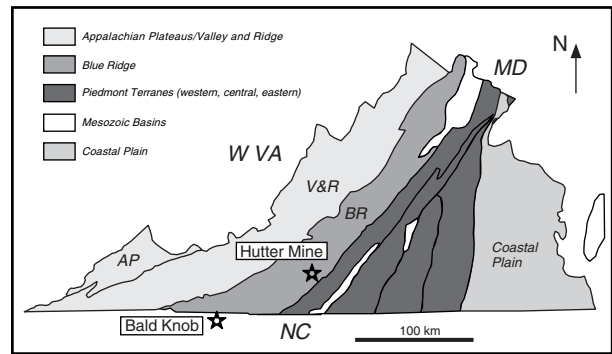


**FIGURE 1.** Generalized map of Virginia, showing the geologic provinces and indicating the locations of the Hutter Mine (this report) and the Bald Knob locality, Sparta, North Carolina (Simmons et al. 1981) within the eastern Blue Ridge province.

1907; Furcron 1935; Espenshade 1954). Iron oxide minerals (both magnetite and hematite) and barite occur in layered deposits that are generally concordant with regional structures and have been folded and metamorphosed with surrounding rocks. Barite is invariably associated with marble, occurring both as massive layers beneath, or as nodules within, marble (Watson 1907).

The Hutter Mine, one of a series of iron mines in the area, operated for about 25 years after the Civil War and ceased operation in 1903. It exploited a thin seam of magnetite ore with an associated thin layer of weathered Mn-rich material (umber) (Watson 1907). Unfortunately, no outcrop remains and the mine was entirely underground (and all subsurface workings have been filled in), so all sampling is from heavily overgrown mine dumps. In 1996, abandoned-mine reclamation operations exposed a single 100 m<sup>2</sup> mine dump of Mn-rich material that was apparently discarded during mining for iron ore. All of our samples of Mn minerals from the deposit are from this single dump, and thus lack context within the original deposit, although some larger samples such as the one discussed here preserve evidence of layering and reaction zones. Further details of the history and general character of the Hutter Mine deposit may be found in Beard et al. (2002).

## METAMORPHIC GRADE AND PHYSICAL CONDITIONS

The pressure and temperature conditions at the peak of amphibolite-facies regional metamorphism at the Hutter Mine were evaluated to constrain conditions of formation of the unusual minerals in the deposit, including kinoshitalite. Fortunately, large blocks of pelitic schist were excavated in the mining operations and were found mixed with ore samples in the mine dumps. A representative schist sample (VMNH no. 604) contains the assemblage quartz-plagioclase-muscovite-biotite-garnet-chlorite-sillimanite (fibrolite)-tourmaline-graphite-ilmenite-pyrrhotite. The sample also contains 1 or 2 modal percent of a blocky pleochroic blue-green mineral that was initially suspected to be chloritoid but which turned out upon microprobe analysis to be aluminiferous ferroschermakite. The coexistence in the schist of intermediate plagioclase ( $\text{An}_{42}$ ) and

calcic amphibole indicates a calc-pelitic tendency.

Fe-Mg exchange thermometry using garnet ( $\text{alm}_{81}\text{py}_{7}\text{sp}_{6}\text{gr}_{6}$ ) and biotite ( $F/M = 0.656$ ) yields  $575\text{ }^{\circ}\text{C}$  (Holdaway 2000) and GASP barometry using the same garnet as well as plagioclase ( $\text{An}_{42}$ ) gives 4.2 kbar (Holdaway 2001) at that temperature. Using THERMOCALC (Holland and Powell 1998), the intersection of the grt-bt Fe-Mg exchange and GASP net-transfer equilibria was calculated at  $580\text{ }^{\circ}\text{C}$  and 3.9 kbar. We therefore accept the conditions of regional metamorphism and equilibration of the ore minerals at the Hutter Mine as approximately  $575\text{ }^{\circ}\text{C}$  and 4 kbar. The  $P$ - $T$  estimate is consistent with the position of the observed metapelitic mineral assemblage on an appropriate petrogenetic grid (cf., Spear 1993), and is similar to  $P$ - $T$  conditions proposed for the Bald Knob locality (Winter et al. 1981).

One of the key minerals in the Hutter Mine Mn-ore assemblage that enables estimation of ambient fluid composition and oxygen fugacity during metamorphism is the rare mineral manganosite,  $\text{MnO}$ , which coexists with hausmannite ( $\text{Mn}_3\text{O}_4$ ) and Ca-Mn carbonates at the Hutter Mine locality. The apparently stable occurrence of manganosite at  $575\text{ }^{\circ}\text{C}$  at the Hutter Mine may be attributed to metamorphism in the presence of a  $\text{CO}_2$ -poor (water-rich) fluid. Local infiltration of an  $\text{H}_2\text{O}$ -rich metamorphic fluid into the Mn-marble probably led to localized decarbonation of Mn-carbonates. The lack of detailed geologic context for the manganosite-bearing sample makes it difficult to interpret how a decarbonation reaction might be related to other reaction-zone phenomena at the Hutter Mine, including skarn development in the sample in which kinoshitalite occurs.

Oxygen fugacity, at least at the time of manganosite formation, is tightly constrained in the Hutter Mine rocks by the stable coexistence of manganosite and hausmannite (Beard and Tracy 2002), i.e., it must lie along the manganosite-hausmannite oxygen buffer. This places the  $T$ - $f_{\text{O}_2}$  conditions well within the magnetite stability field (Huebner 1967, 1976), and is thus consistent with the presence of extensive magnetite ore at the Hutter Mine locality.

### SAMPLE DESCRIPTION

The single mine-dump sample that has so far yielded kinoshitalite (VMNH no. 603) is a composite layered sample that preserved an apparent reaction front between skarn and marble that developed during metamorphism (Fig. 2). The mineral assemblage in the lighter-colored marble is kutnahorite + manganosite + alleghanyite + sonolite + aluminous jacobite + kinoshitalite + alabandite. In this layer, kinoshitalite is scarce (<1%) and very wispy and fine-grained (<0.3 mm) (Fig. 3A). In contrast, large (1–2 mm), well-formed kinoshitalite crystals make up 5–10% of the skarn near the reaction front (Fig. 3B). The skarn assemblage includes minor kutnahorite + tephroite + manganumite + spessartine + kinoshitalite + jacobite + manganosite magnetite. Representative microprobe analyses of minerals in the skarn and marble assemblages are given in Table 1.

Kinoshitalite in both zones has similar pleochroism (tan to orange-brown), but the larger crystals in the skarn have considerably more intense color, possibly due either to their sub-

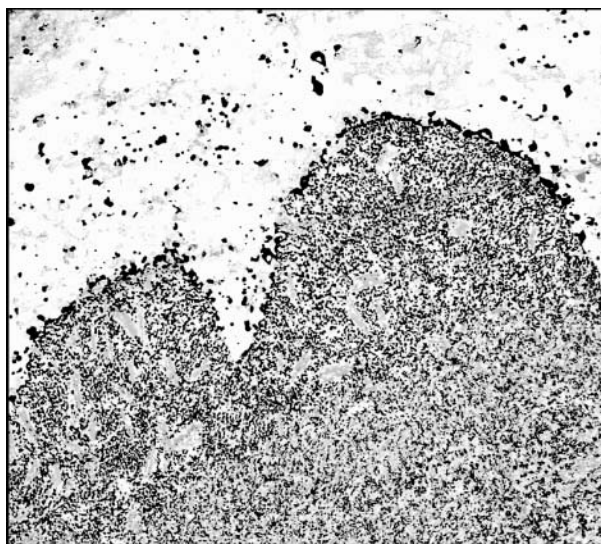


**FIGURE 2.** Low-magnification photomicrograph of thin section VMNH no. 603 showing manganosite marble (top) and silicate-oxide skarn (bottom), separated by a reaction front with concentration of opaque large aluminous jacobite grains. The marble is dominated by pale, transparent Ca-Mn carbonate, but carbonate is scarce in the skarn. Note the large kinoshitalite flakes in the skarn, particularly at the lower left of the photomicrograph. Width of field of view of the photograph is 25 mm.

stantially higher  $(\text{Mn} + \text{Fe})/(\text{Mn} + \text{Fe} + \text{Mg})$  and Ti contents (Table 2) or to small variations in  $\text{Fe}^{2+}/\text{Fe}^{3+}$ .

### MINERAL CHEMISTRY

Minerals were analyzed on a Cameca SX50 electron probe microanalyzer at the Department of Geological Sciences, Virginia Tech. All analyses were done at 15 kV accelerating potential and 20 nA beam current. Kinoshitalite and carbonate analyses were done using an approximately  $5\text{ }\mu\text{m}$  spot size; other minerals were analyzed with an approximately  $1\text{ }\mu\text{m}$  spot. A combination of natural and synthetic silicates and oxides was used as standards, including: Amelia albite (Na, Si), Marjalahti olivine (Mg), norbergite (F), synthetic chlor-apatite (Ca, Cl), Benson orthoclase (K), synthetic Ba-apatite (Ba), rutile (Ti),  $\text{Cr}_2\text{O}_3$  (Cr),  $\text{MnO}$  (Mn), and  $\text{Fe}_2\text{O}_3$  (Fe). Minerals were not routinely analyzed for Sr because WDS scans of the  $\text{SrL}\alpha$  peak were run on micas and carbonates, and no Sr was found.

Approximately 70 microprobe analyses of kinoshitalites were made in both the skarn and marble layers of sample VMNH no. 603. Representative analyses of kinoshitalite that cover the range of observed Ba contents are given in Table 2. The structural formulae were recalculated to 22 positive cation charges on an anhydrous basis (equivalent to 11 O atoms for a fluorine- and chlorine-free mica), as the large and variable fluorine content rendered it impossible to select a unique number of oxygen atoms per formula unit.

Examination of the data in Table 2 reveals compositional contrasts between kinoshitalites in the two lithologies at the Hutter Mine, many of which can be linked genetically to the

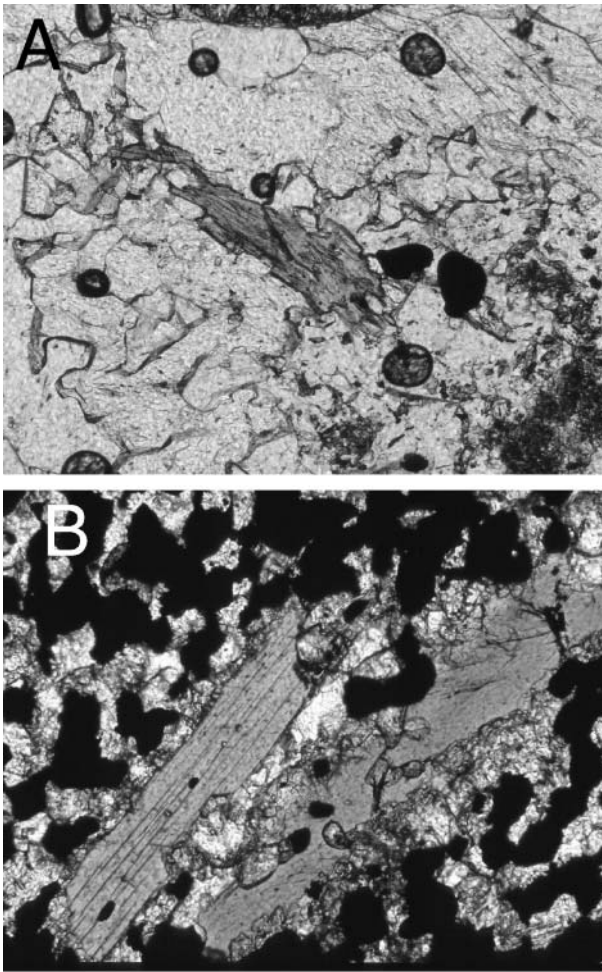


**FIGURE 3.** Photomicrographs of typical kinoshitalite in marble (A) and in skarn (B). In A, the small kinoshitalite crystal at the center is surrounded by Ca-Mn carbonate and sonolite, with two rounded grains of opaque jacobsite. In B, larger crystals of kinoshitalite occur in a matrix rich in jacobsite and Mn-magnetite, with Mn-humites, spessartine-rich garnet and minor carbonate. Field of view of A is 0.5 mm. Field of view of B is 2.0 mm.

origin of the skarn as a reaction zone between manganous marble and country rock (probably metapelite). Mean total  $\text{Al}_2\text{O}_3$  (from all analyses) in kinoshitalite from marble (KM) is 19.50 wt% vs. 21.66 in skarn (KS), in contrast to mean BaO of 21.05 in KS vs. 26.27 in KM. The more Ba-rich mica, with higher (Ba + Ca) content, would normally be expected to be more aluminous through the coupled exchange vector (Ba,Ca)AlK<sub>1</sub>Si<sub>1</sub>. However, KS has a very different and higher extent of total Tschermak component,  $^{\text{VI}}\text{Al}^{\text{VI}}\text{Al}(\text{Fe},\text{Mg},\text{Mn})_{-1}\text{Si}_{-1}$ , than KM. On a formula basis of 24 anions, mean total octahedral Fe + Mg + Mn is 5.894 in KM vs. 5.424 in KS. This difference of 0.470 almost perfectly balances the difference in calculated octahedral (Al + Cr + Fe<sup>3+</sup> + 2Ti) - 0.138 in KM vs. 0.688 in KS—when corrected for the tetrahedral Al difference that is not accounted for by the brittle-mica substitution.

Other compositional contrasts for kinoshitalite in the two

environments are consistent with the model of skarn originating as a reaction zone. Mean contents of Ti, Mn, and calculated Fe<sup>3+</sup> are substantially higher in skarn kinoshitalite, whereas contents of Ca, Ba, Mg, and F are much higher in marble, as is the mean Mg/(Mg + Fe + Mn).

The larger kinoshitalite crystals in the skarn may have grown continuously during diffusive transport of various components, so we carefully examined several for compositional zonation with closely spaced microprobe traverses and with two-dimensional X-ray intensity (analog compositional) maps. No evidence of even subtle zoning was found in any of the examined crystals.

## DISCUSSION

### Chemical compositions of kinoshitalites

Kinoshitalites in both marble and skarn of sample VMNH no. 603 show substantial variability in chemistry, although this variability is considerably greater within the skarn: wt% BaO in skarn kinoshitalite ranges from 18 to 23 wt%, compared with a range in marble from 26 to 28 wt% BaO. The obvious first issue that arises is whether this variability shows any systematic areal pattern that might reflect variable elemental diffusive mobility during formation of the reaction skarn. Using data on X-Y positions of individual probe analyses in the thin section relative to the obvious reaction front (see Fig. 2), we have been unable to deduce such a pattern. However, any patterns that do exist may be complicated by an expected geometrical complexity of the reaction front in three dimensions.

Starting from an ideal phlogopite composition of  $\text{K}_2\text{Mg}_6\text{Al}_2\text{Si}_6\text{O}_{20}(\text{OH})_4$  (Bailey 1984), there are several trioctahedral mica compositional exchange vectors (Guidotti 1984) that operate in the kinoshitalite from the Hutter Mine:

1. "Wonesite" or sodium phlogopite =  $^{\text{A}}\text{NaK}_{-1}$
2. "clintonite" =  $^{\text{A}}\text{Ca}^{\text{IV}}\text{AlK}_{-1}\text{Si}_{-1}$
3. "kinoshitalite" =  $^{\text{A}}\text{Ba}^{\text{IV}}\text{AlK}_{-1}\text{Si}_{-1}$
4. Al-Tschermak =  $^{\text{VI}}\text{Al}^{\text{IV}}\text{Al}(\text{Fe},\text{Mg},\text{Mn})_{-1}\text{Si}_{-1}$
5. Ferri-Tschermak =  $\text{Fe}^{3+\text{IV}}\text{Al}(\text{Fe},\text{Mg},\text{Mn})_{-1}\text{Si}_{-1}$
6. Ti-Tschermak =  $\text{Ti}^{\text{IV}}\text{Al}_2(\text{Fe},\text{Mg},\text{Mn})_{-1}\text{Si}_{-2}$
7. Fluor-mica =  $\text{F}(\text{OH})_{-1}$
8. Chlor-mica =  $\text{Cl}(\text{OH})_{-1}$

The first three of the above exchanges may be referred to as "mica" exchanges because they involve the mica interlayer site (A site). The second three are variants of the coupled Tschermak exchange involving both tetrahedral and octahedral sites, and the last two involve only OH<sup>1-</sup>.

**Exchanges involving the interlayer-cation (A) site.** Substantial variations in interlayer site occupancy occur among the cations K, Ba, and Ca; by contrast Na content (exchange 1) is uniformly low. Figure 4 illustrates the very different interrelationships between K, Ba and Ca in marble and skarn kinoshitalites (exchanges 2 and 3). The group of marble kinoshitalite analyses shows essentially binary solid solution between Ba and Ca, ranging up to 11 percent Ba replaced by Ca, with virtually no K, whereas the skarn kinoshitalite analyses show the opposite—solid solution between Ba and K ranging from 5 to 25 percent Ba replaced by K, with little or no Ca. These relationships are consistent with bulk compositional con-

**TABLE 1.** Representative compositions of minerals in skarn and marble

	Skarn				Marble		
	Tephro- roite	Mn- Humite	Garnet	Jacob- site	Sonolite	Spinel 1	Spinel 2
SiO <sub>2</sub>	29.91	26.90	36.45	0.00	27.14	0.00	0.00
TiO <sub>2</sub>	0.04	0.10	0.01	1.04	0.12	0.73	0.87
Al <sub>2</sub> O <sub>3</sub>	0.01	0.00	20.46	2.57	0.02	21.52	6.93
FeO	3.58	2.32	0.97	61.38	2.40	41.48	57.13
MnO	64.22	65.16	39.56	26.17	65.82	30.14	27.04
MgO	2.04	3.17	0.13	0.11	2.83	0.46	0.18
ZnO	0.00	0.00	0.01	0.45	0.00	0.48	0.31
CaO	0.14	0.17	3.13	0.00	0.07	0.00	0.00
F	0.00	2.46	0.00	0.00	1.91	0.00	0.00
-F = O	0.00	1.04	0.00	0.00	0.80	0.00	0.00
SUM	99.94	99.24	100.71	91.76	99.51	94.87	92.50
no. Ox	4	13	12	4	17	4	4
Si	0.993	3.016	2.977	0.000	3.960	0.000	0.000
Ti	0.001	0.008	0.000	0.030	0.013	0.019	0.025
Al	0.000	0.000	1.969	0.117	0.003	0.872	0.306
Fe <sup>2+</sup>	0.099	0.218	0.066	0.159	0.293	0.108	0.149
Fe <sup>3+</sup>	—	—	—	1.820	—	1.086	1.642
Mn	1.805	6.184	2.735	0.854	8.129	0.878	0.858
Mg	0.101	0.530	0.015	0.006	0.615	0.024	0.010
Zn	0.000	0.000	0.001	0.013	0.000	0.012	0.009
Ca	0.000	0.020	0.274	0.000	0.011	0.000	0.000
F	0.000	0.872	0.000	0.000	0.881	—	—
Cation Sum	3.005	9.976	8.038	3.000	13.025	3.000	3.000

\* Calculated in spinels using assumption of stoichiometry and charge balance.

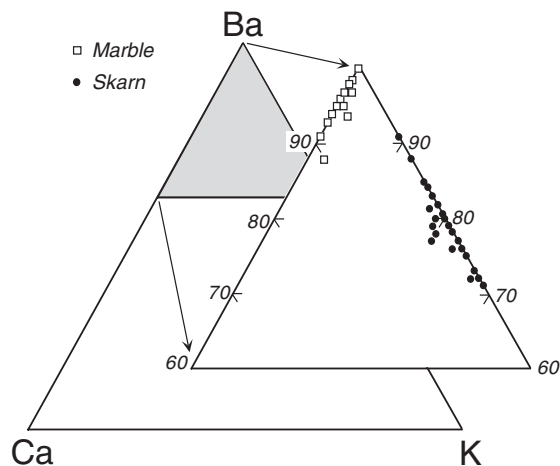


**FIGURE 4.** Ternary plot of the Ba-rich corner of the Ba-Ca-K mica ternary, showing proportional occupancy of Ba, Ca, and K in the A site of kinoshitalite from skarn and marble zones in VMNH no. 603. The distribution of skarn data points indicates variation mostly of K and Ba, with minor and relatively constant amounts of Ca and Na in the A-site. Marble data points indicate a very restricted range of K in these kinoshitalites, and a generally higher proportion of Ba.

**TABLE 2.** Representative kinoshitalite analyses from the Hutter Mine

Analysis no.	1-28	1-8	1-21	1-4	Ave (35)	2-11	2-32	2-8	Ave (27)
Rock type*	S	S	S	S	S	M	M	M	M
SiO <sub>2</sub>	22.64	22.23	21.52	21.38	21.92	22.03	22.56	22.16	21.98
TiO <sub>2</sub>	0.33	0.34	0.49	0.43	0.46	0.14	0.07	0.12	0.11
Al <sub>2</sub> O <sub>3</sub>	22.03	22.12	21.35	22.14	21.52	19.53	19.73	20.04	20.03
Cr <sub>2</sub> O <sub>3</sub>	0.16	0.15	0.13	0.11	0.16	0.00	0.00	0.04	0.01
FeO*	3.58	3.52	3.86	3.46	3.85	2.06	2.42	2.09	2.61
MnO	11.59	10.83	11.23	10.98	11.51	7.07	6.57	7.01	8.04
MgO	12.85	13.51	13.17	13.18	12.62	16.75	17.25	17.09	15.88
CaO	0	0.27	0.00	0.00	0.04	0.66	0.40	0.67	0.29
BaO	19.43	21.44	22.15	23.20	20.94	25.92	26.04	27.90	25.39
Na <sub>2</sub> O	0.05	0.05	0.05	0.05	0.06	0.05	0.06	0.05	0.05
K <sub>2</sub> O	2.38	1.75	1.54	1.41	1.75	0.00	0.03	0.01	0.30
F	0.88	1.02	1.19	1.01	0.99	2.18	2.28	1.99	1.99
Cl	0.07	0.07	0.09	0.08	0.08	0.03	0.04	0.03	0.04
minus O = F + Cl	0.39	0.45	0.52	0.44	0.44	0.92	0.97	0.84	0.85
SUM	95.60	96.85	96.25	96.99	95.47	95.50	96.48	98.36	95.88
<b>Formulas on the basis of 22 cation (+) charges</b>									
Si	1.976	1.935	1.913	1.888	1.945	1.980	1.999	1.953	1.970
Al	2.024	2.065	2.087	2.112	2.055	2.012	2.001	2.029	2.030
Tet Sum	4.000	4.000	4.000	4.000	4.000	4.000	4.000	4.000	4.000
Al	0.215	0.175	0.114	0.162	0.166	0.000	0.001	0.000	0.033
Ti	0.021	0.022	0.032	0.028	0.030	0.009	0.005	0.008	0.007
Cr	0.011	0.010	0.009	0.008	0.011	0.000	0.000	0.003	0.001
Fe	0.258	0.253	0.282	0.252	0.282	0.151	0.174	0.150	0.190
Mn	0.847	0.788	0.832	0.810	0.854	0.523	0.479	0.510	0.595
Mg	1.653	1.730	1.718	1.712	1.647	2.182	2.214	2.189	2.068
Oct Sum	3.005	2.978	2.988	2.973	2.991	2.866	2.874	2.860	2.895
Ca	0.000	0.025	0.000	0.000	0.004	0.062	0.037	0.062	0.027
Ba	0.657	0.722	0.759	0.792	0.719	0.888	0.879	0.939	0.869
Na	0.008	0.008	0.008	0.008	0.010	0.008	0.010	0.008	0.009
K	0.262	0.192	0.172	0.157	0.195	0.000	0.003	0.001	0.033
A Sum	0.927	0.947	0.940	0.957	0.928	0.958	0.929	1.010	0.939
F	0.243	0.281	0.334	0.282	0.279	0.620	0.639	0.554	0.565
Cl	0.010	0.010	0.014	0.012	0.012	0.005	0.006	0.004	0.006
OH†	0.747	0.709	0.652	0.706	0.710	0.376	0.355	0.441	0.429
Ba/A tot	0.708	0.762	0.808	0.827	0.774	0.927	0.946	0.930	0.926
Mn/(Mn + Fe + Mg)	0.307	0.284	0.294	0.292	0.307	0.183	0.167	0.179	0.208
Mg/(Mg + Fe + Mn)	0.599	0.624	0.607	0.617	0.592	0.764	0.772	0.768	0.725

\* S = skarn; M = marble.

† Calculated from 2 - (F + Cl).

siderations in both marble and skarn. Although not shown in this paper, a plot of  $^A X_{Ba}$  vs. Ca/22 cation charges shows a strongly linear behavior.

Figure 5 illustrates the correlation between A-site occupancy of divalent cations and tetrahedral-site occupancy of Al due to the coupled nature of exchanges 2 and 3. The ideal mica vector with a slope of 1 is shown, as is the kinoshitalite end-member. The marble kinoshitalite analyses fall relatively close to the ideal mica vector whereas the skarn kinoshitalite analyses diverge significantly from this vector. In other words, skarn kinoshitalites are much lower in Si and higher in  $^{IV}Al$  than is justified by their Ba + Ca contents. Deviation of skarn kinoshitalites from the ideal mica vector is due to significantly higher total Tschermak content of skarn kinoshitalites, illustrated by the Tschermak vector shown in Figure 5.

**Exchanges involving octahedral cations.** The three model Tschermak exchange vectors (exchanges 4, 5, and 6), operating in a positive sense, involve substitution of higher-valent cations (Al,  $Fe^{3+}$ , Ti) into octahedral sites normally occupied by divalent cations in trioctahedral micas. The skarn layer is notably higher in Al and Ti content than the marble, and calculated  $Fe^{3+}$  content of kinoshitalite is higher than for marble, and this results in a substantially higher Tschermak content of skarn kinoshitalites than of marble kinoshitalites: ( $^{VI}Al + Fe^{3+} + Ti$ ) occupy 2.0% of total octahedral sites in KM vs. 10.2% in skarn kinoshitalites.

The Tschermak content of kinoshitalites in marble shows very little variation compared to that in kinoshitalite from skarn. There are no discernible correlations between total Tschermak content of any individual skarn kinoshitalite crystal and either

other compositional parameters (e.g., total Mn, ratios of Mn, Mg, or Fe to other divalent cations) or with position within the skarn zone.

**Anion exchanges.** Fluorine substitution for OH is significant in all the Hutter Mine kinoshitalites: 0.65 to 1.5 wt% F in skarn and 1.9 to 2.5 wt% F in the marble, which correlates to between 12 and 37 percent of the OH site occupied by F. The most obvious correlation of the F content in both marble and skarn kinoshitalites is with  $Mg/(Mg + Fe + Mn)$  (Fig. 6), with significantly higher F in the more magnesian kinoshitalites in marble. This relationship suggests that there may be a Mn-F avoidance effect similar to the known Fe-F avoidance. The Cl content of both types of kinoshitalite is low and relatively uniform.

### Implications of kinoshitalite compositions

The major first-order control of compositional variation within the Hutter Mine kinoshitalites appears to be bulk compositions: marble-zone vs. skarn-zone. In the former group (marble kinoshitalites), the A-site is almost entirely occupied by divalent cations Ca and Ba, with virtually no K or Na, resulting in a mica that closely approximates an ideal brittle-mica composition. Substitution of Ba by Ca is quite limited, but within this narrow range, there is substantial variability in Ba/Ca ratio in the A site. In the latter group (skarn kinoshitalites), the A-site is occupied by Ba and K, with virtually no Ca or Na, resulting in a mica that is dominantly barian but which has between 16 and 27 percent manganese K-phlogopite component. Thus the two types of kinoshitalite in this composite sample are effectively a Ba-Ca near-binary variety in marble

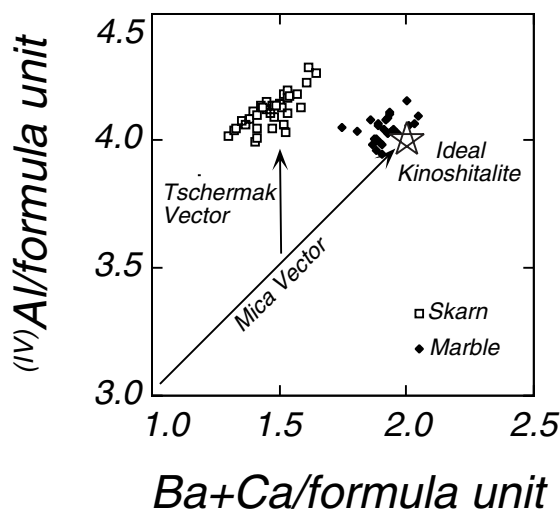


**FIGURE 5.** Plot of  $^{IV}Al$  per formula unit (based on 22 positive cation charges) as a function of total divalent cation (Ba + Ca) occupancy of kinoshitalite A-sites. An ideal composite brittle mica exchange vector is shown as is the location of a brittle-mica end-member (in this case, labeled *kinoshitalite*). Note that kinoshitalite from the marble falls close to the ideal mica vector, and also close to the kinoshitalite end-member, whereas kinoshitalite from skarn diverges significantly due both to greater  $^{IV}Al$  as a Tschermak component and to substantial replacement of Ba by K.

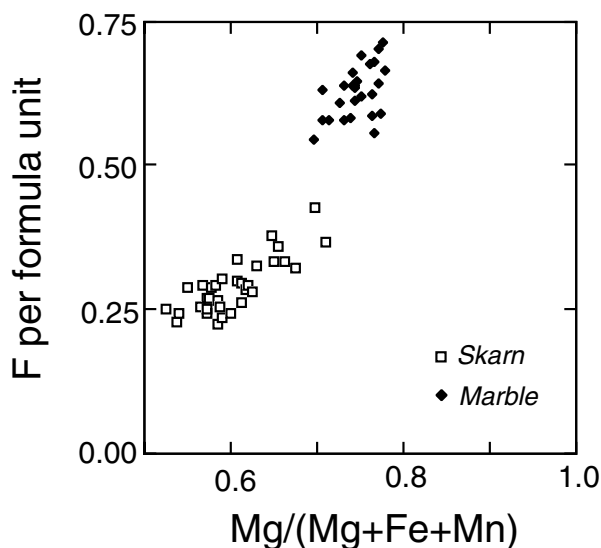


**FIGURE 6.** Fluorine content per formula unit (22 cation positive charges) of kinoshitalites as a function of  $Mg/(Mg + Fe + Mn)$  in the octahedral sites. Note the positive correlation and the essentially non-overlapping ranges of  $Mg/(Mg + Fe + Mn)$  and F content in the two groups of kinoshitalites from skarn and marble.

and a Ba-K variety in skarn.

**Tschermak substitution.** An important secondary effect related to the two compositional environments is the total Tschermak content (octahedral Al + Ti + Fe<sup>3+</sup>, coupled with tetrahedral Al), which averages 2% in kinoshitalite from the marble and 10% in the skarn. The likely control of the higher Tschermak content in skarn kinoshitalites is the higher bulk Al<sub>2</sub>O<sub>3</sub> and TiO<sub>2</sub> content of the skarn, along with a slightly higher *f*<sub>O<sub>2</sub></sub> (Beard and Tracy 2002).

Calcic brittle micas are not normally so deficient in Tschermak content (mainly Al-Tschermak) compared with biotites, even in relatively low-Al environments. For example, for the seven clintonite analyses tabulated in Deer et al. (1962), the range of <sup>VI</sup>(Al + Ti + Fe<sup>3+</sup>) is 24 to 26% of total octahedral occupancy, and most of this was derived from <sup>VI</sup>Al, even though most listed samples were from marbles. Other typical reported values for <sup>VI</sup>(Al + Ti + Fe<sup>3+</sup>) content in clintonite are: 24.8% (Takeuchi and Sadanaga 1966), 36% (Akhundov et al. 1961), 23% (Alietti et al. 1997), and 21–27% (MacKinney et al. 1988). No reports of less than 20% occupancy of octahedral sites in clintonite by tri- and quadrivalent cations were found in a literature search, and one model for clintonite tetrahedral-layer composition is SiAl<sub>3</sub> (Guggenheim 1984), compared to Si<sub>2</sub>Al<sub>2</sub> for ideal brittle mica with no Tschermak substitution.

As indicated by the data in this paper, the extent of Tschermak substitution in barian brittle micas must differ systematically from that in calcic brittle micas, although this point was not addressed by Guggenheim (1984) in his review of brittle-mica crystal chemistry. The <sup>VI</sup>(Al + Ti + Fe<sup>3+</sup>) content in analyzed kinoshitalites reported by Gnos and Armbruster (2000) is 1.5 to 2% of total octahedral occupancy, and in analyses reported by Frimmel et al. (1995) for ferrokinoshitalite, this value ranges from 7 to 10%, compared to our values of 2% in marble and 10% in skarn. Solie and Su (1987) reported this value as 4.5 to 6% for barian green mica from calc-silicate, and Guggenheim and Kato (1984) reported it as 9% in kinoshitalite.

**Fluorine substitution in the hydroxyl site.** Table 2 and Figure 6 illustrate a second major compositional contrast between marble and skarn kinoshitalites in sample VMNH no. 603. The F content of both groups is similar to that of most other reported kinoshitalites, but the F content of the marble kinoshitalite is substantially higher (mean F of 2.2 wt%, or 31% of the hydroxyl sites) than that of skarn kinoshitalite, (1.0 wt% or 14%). In contrast, F contents of other reported kinoshitalites are widely variable: e.g., 1.3 wt% or 16% (Gnos and Armbruster 2000), 2.7 wt% or 34% (Solie and Su 1987), and 2.2–4.0 wt% or 30–56% (Frimmel et al. 1995).

### Petrogenesis of kinoshitalite at the Hutter Mine

Because there is no direct petrographic evidence for a kinoshitalite-forming reaction in the Hutter Mine sample, possible reactions must be constructed from documented or potential reactant phases. The restriction of kinoshitalite to upper-middle amphibolite-facies conditions or higher in this and other occurrences suggests that peak or near-peak metamorphic minerals are the likely reactants.

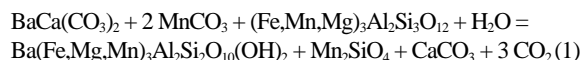
The kinoshitalite A-sites contain Ba, Ca, and K. In both the skarn and marble lithologies, there is no barian mineral other

than kinoshitalite itself, so the initial source of Ba must be in a mineral that was entirely consumed during reaction. The only Ba minerals found anywhere in the deposit are sulfate (barite = BaSO<sub>4</sub>) and carbonate [BaCa(CO<sub>3</sub>)<sub>2</sub> = likely barytocalcite]. Because no S- or SO<sub>4</sub>-bearing mineral currently occurs in the skarn, we suggest BaCa(CO<sub>3</sub>)<sub>2</sub> as a Ba source. However, alabandite (MnS) occurs in the marble, and may be a product mineral that incorporates reduced S from the reaction, so we cannot preclude the presence of barite in the marble prior to reaction.

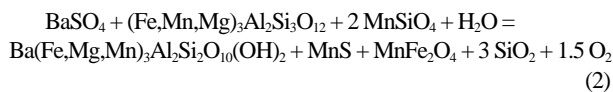
As with Ba, there is no potassic mineral in either skarn or marble but, because the skarn is an obvious fluid-mediated reaction zone between ore and country rock, it is possible, even likely, that K was introduced metasomatically. In any case, K is typically only a minor constituent of kinoshitalite in skarn and virtually absent in marble. Various Ca-bearing carbonate minerals occur in both lithologies and are likely sources for Ca, particularly in the marble.

The octahedral-layer constituents Fe, Mn, and Mg occur in abundance in both skarn and marble in silicates (Mn-humites, tephroite, garnet) and in oxides (jacobsonite, magnetite, galaxite). The skarn is much more aluminous than the marble, which may help to explain the considerably greater abundance of kinoshitalite there.

On the basis of the above reasoning, two highly generalized hypothetical reactions may be proposed for kinoshitalite formation at the Hutter Mine, one assuming an initial source of Ba in a carbonate and the second assuming Ba in a sulfate. Both Ba-carbonate and Ba-sulfate have been identified in other samples at the Hutter Mine. The first involves BaCa(CO<sub>3</sub>)<sub>2</sub>:



and the second involves barite:



Both reactions are strikingly simple, largely because they are multivariant and involve several compositionally complex solid solutions. Because of their generalized and hypothetical character, balancing may not be terribly significant. For example, in reaction 1, the Mn-rich silicate product could also be one of the Mn-humite minerals, rather than tephroite, and a complex Ca-Mn-Mg carbonate mineral such as kutnahorite might replace rhodochrosite as a reactant. But in the absence of any additional constraints on the reaction mechanism, we present these two hypothetical reactions as possible scenarios for the formation of kinoshitalite at *T* > 500 °C. In any case, whatever reaction produced kinoshitalite from a Ba-bearing precursor mineral must have completely exhausted that precursor mineral, as no Ba mineral other than kinoshitalite has been observed in sample VMNH no. 603.

### ACKNOWLEDGMENTS

The authors thank W.S. Henika for help with field work and sample collection for this study, as well as for sharing his wisdom on the regional geology of the Virginia Piedmont. Eric Essene, Jerry Gibbs, Nancy Ross, Ross Angel, and

Paul Ribbe are gratefully acknowledged for many very helpful discussions on mineralogy and crystal chemistry of manganese minerals and their phase-equilibrium implications. Eric Essene provided an extraordinarily thorough and helpful review of this paper. Brent Owens and two anonymous reviewers are also thanked for comments that aided in improving the manuscript.

## REFERENCES CITED

- Akhundov, Y.A., Mamedov, K.S., and Belov, N.V. (1961) The crystal structure of brandisite. *Doklady Akademia Nauk SSSR, Earth Sciences Sections*, 137, 438–440.
- Alietti, E., Brigatti, M.F., and Poppi, L. (1997) Clintonite-1M: crystal chemistry and its relationships to closely associated Al-rich phlogopite. *American Mineralogist*, 82, 936–945.
- Bailey, S.W. (1984) Crystal chemistry of the true micas. In S.W. Bailey, Ed., *Micas*, 13, 13–60. Reviews in Mineralogy, Mineralogical Society of America, Washington, D.C.
- Beard, J.S. and Tracy, R.J. (2002) Spinel and other oxides in Mn-rich rocks from the Hutter Mine, Pittsylvania County, Virginia, USA, with implications for solvus relations among jacobite, galaxite, and magnetite. *American Mineralogist*, 86, 690–698.
- Beard, J.S., Tracy, R.J., and Henika, W.S. (2002) Minerals of the Hutter Mine, a new manganese-barium mineral locality in northern Pittsylvania County, Virginia. *Rocks and Minerals*, 77, 320–325.
- Bol, L.C.G.M., Bos, A., Sauter, P.C.C., and Jansen, J.B.H. (1989) Barium-titanium-rich phlogopites in marbles from Rogaland, southwest Norway. *American Mineralogist*, 74, 439–447.
- Brigatti, M.F. and Poppi, L. (1993) Crystal chemistry of Ba-rich trioctahedral micas 1M. *European Journal of Mineralogy*, 5, 857–871.
- Bücher-Nurminen, K. (1982) Mechanism of mineral reactions inferred from textures of impure dolomitic marbles from East Greenland. *Journal of Petrology*, 23, 325–343.
- Chabu, M. and Baulgé, J. (1992) Barium feldspar and muscovite from Kingushi Zn-Pb-Cu deposit, Shaba, Zaire. *Canadian Mineralogist*, 30, 1143–1152.
- Dasgupta, S., Chakraborti, S., Sengupta, P., Bhattacharya, P.K., and Banerjee, H. (1989) Compositional characteristics of kinoshitalite from the Sausar Group, India. *American Mineralogist*, 74, 200–202.
- Deer, W.A., Howie, R.A., and Zussman, J. (1962) *Rock-Forming Minerals*, vol. 3: Sheet Silicates, 270 p. Longmans, Green and Co., Ltd., London.
- Dunning, G.E. and Cooper, J.F. Jr. (1999) Barium silicate minerals from Trumbull Peak, Mariposa County, California. *Mineralogical Record*, 30, 411–417.
- Edgar, A.D. (1992) Barium-rich phlogopite and biotite from some Quaternary alkali mafic lavas, West Eifel, Germany. *European Journal of Mineralogy*, 4, 321–330.
- Espenshade, G.H. (1954) Geology and mineral deposits of the James River—Roanoke River manganese district, Virginia. U.S. Geological Survey Bulletin 1008, Washington, D.C.
- Filut, M.A., Rule, A.C., and Bailey, S.W. (1985) Crystal structure refinement of anandite-2Or, a barium- and sulfur-bearing trioctahedral mica. *American Mineralogist*, 70, 1298–1308.
- Frimmel, H.E., Hoffmann, D., Watkins, R.T., and Moore, J.M. (1995) An Fe analogue of kinoshitalite from the Broken Hill massive sulfide deposit in the Namaqualand Metamorphic Complex, South Africa. *American Mineralogist*, 80, 833–840.
- Frondel, C. and Ito, J. (1967) Barium-rich phlogopite from Långban, Sweden. *Arkiv för Mineralogi och Geologi*, 4, 445–447.
- Furcron, A.S. (1935) James River iron and marble belt, Virginia, 65 p. Virginia Geological Survey Bulletin 39, Charlottesville, Virginia.
- Gaspar, J.C. and Wyllie, P.J. (1982) Barium phlogopite from the Jacupiranga carbonatite, Brazil. *American Mineralogist*, 67, 997–1000.
- Glassley, W.E. (1975) High-grade regional metamorphism of some carbonate bodies: significance for the orthopyroxene isograd. *American Journal of Science*, 275, 1133–1163.
- Gnos, E. and Armbruster, T. (2000) Kinoshitalite,  $\text{Ba}(\text{Mg})_3(\text{Al}_2\text{Si}_2)_{10}(\text{OH},\text{F})_2$ , a brittle mica from a manganese deposit in Oman: paragenesis and crystal chemistry. *American Mineralogist*, 85, 242–250.
- Guggenheim, S. (1984) The brittle micas. In Sturges W. Bailey, Ed., *Micas*, 13, 61–104. Reviews in Mineralogy, Mineralogical Society of America, Washington, D.C.
- Guggenheim, S. and Frimmel, H.E. (1999) Ferrokinoshitalite, a new species of brittle mica from the Broken Hill Mine, South Africa; structural and mineralogical characterization. *Canadian Mineralogist*, 37, 1445–1452.
- Guggenheim, S. and Kato, T. (1984) Kinoshitalite and Mn phlogopites: Trial refinements in subgroup symmetry and further refinement in ideal symmetry. *Mineralogical Journal*, 12, 1–5.
- Guidotti, C.V. (1984) Micas in metamorphic rocks. *Mineralogical Society of America, Reviews in Mineralogy*, 13, 357–468.
- Harlow, G.E. (1995) Crystal chemistry of barium enrichment in micas from metasomatized inclusions in serpentinite, Montagua fault zone, Guatemala. *European Journal of Mineralogy*, 7, 775–789.
- Hibbard, J.P., Tracy, R.J., and Henika, W.S. (2003) The Smith River Allochthon: A Southern Appalachian peri-Gondwanan terrane emplaced directly on Laurentia? *Geology*, in press.
- Holdaway, M.J. (2000) Application of new experimental and garnet Margules data to the garnet-biotite thermometer. *American Mineralogist*, 85, 881–892.
- (2001) Recalibration of the GASP geobarometer in light of recent garnet and plagioclase activity models and versions of the garnet-biotite geothermometer. *American Mineralogist*, 86, 1117–1129.
- Holland, T.J.B. and Powell, R. (1998) An internally consistent thermodynamic dataset for phases of petrologic interest. *Journal of Metamorphic Geology*, 16, 309–343.
- Huebner, J.S. (1967) Stability Relations of Minerals in the System Mn-Si-C-O. Ph.D. Dissertation, Johns Hopkins University, 279 p.
- (1976) The manganese oxides—a bibliographic commentary. In D. Rumble, Ed., *Oxide Minerals*, 3, SH 1-SH 17. Reviews in Mineralogy, Mineralogical Society of America, Washington, D.C.
- Lanzirotti, A. and Hanson, G.N. (1997) An assessment of the utility of staurolite in U-Pb dating of metamorphism. *Contributions to Mineralogy and Petrology*, 129, 352–365.
- MacKinney, J.A., Mora, C.I., and Bailey, S.W. (1988) Structure and crystal chemistry of clintonite. *American Mineralogist*, 73, 365–375.
- Mansker, W.L., Ewing, R.C., and Keil, K. (1979) Barian-titanian biotites in nephelinites from Oahu, Hawaii. *American Mineralogist*, 64, 156–159.
- Matsubara, S., Kato, A., Nagashima, A., and Matsuo, G. (1976) The occurrence of kinoshitalite from Hokkejino, Kyoto Prefecture, Japan. *Bulletin of the Natural Science Museum, Series C*, 2, 71–78.
- Pan, Y. and Fleet, M.E. (1991) Barium feldspar and barian-chromian muscovite from the Hemlo area, Ontario. *Canadian Mineralogist*, 29, 481–498.
- Pattiarachi, D.B., Saari, E., and Sahama, T.G. (1967) Anandite, a new barium-iron silicate from Wilagedera, Northwestern province, Ceylon. *Mineralogical Magazine*, 36, 1–4.
- Rice, J.M. (1977) Progressive metamorphism of impure dolomitic limestone in the Marysville aureole, Montana. *American Journal of Science*, 277, 1–24.
- Simmons, W.B., Peacor, D.R., Essene, E.J., and Winter, G.A. (1981) Manganese minerals at Bald Knob, North Carolina. *Mineralogical Record*, 167–171.
- Solie, D.N. and Su, S.-C. (1987) An occurrence of Ba-rich micas from the Alaska Range. *American Mineralogist*, 72, 995–999.
- Spear, F.S. (1993) *Metamorphic Phase Equilibria and Pressure-Temperature-Time Paths*. Mineralogical Society of America Monograph 1, 799 p. Washington, D.C.
- Takeuchi, Y. and Sadanaga, R. (1966) Structural studies of brittle micas. (I). The structure of xanthophyllite refined. *Mineralogical Journal*, 4, 424–437.
- Thompson, R.N. (1977) Primary basalts and magma genesis. III. Alban Hills, Roman comagmatic province, central Italy. *Contributions to Mineralogy and Petrology*, 60, 91–108.
- Tracy, R.J. (1991) Ba-rich micas from the Franklin Marble, Lime Crest and Sterling Hill, New Jersey. *American Mineralogist*, 76, 1683–1693.
- Tracy, R.J., Hibbard, J.P., and Henika, W.S. (2001) Implications of a Cambrian (530 Ma) tectono-thermal event in the Smith River Allochthon, Southern Virginia. *Geological Society of America, Abstracts with Programs*, 33, 262.
- Watanabe, T., Yui, S., and Kato, A. (1970) Metamorphosed bedded manganese deposits of the Noda-Tamagawa Mine. In T. Tatsumi, Ed., *Volcanism and Ore Genesis*, p. 143–152. University of Tokyo Press, Tokyo.
- Watson, T.L. (1907) *Mineral Resources of Virginia*. J.P. Bell, Lynchburg, VA, 618 p.
- Wendlandt, R.F. (1977) Barium-phlogopite from Haystack Butte, Highwood Mountains, Montana. *Carnegie Institution of Washington, Yearbook* 76, 534–539.
- Winter, G.A., Essene, E.J., and Peacor, D.R. (1981) Carbonates and pyroxenoids from the manganese deposit near Bald Knob, North Carolina. *American Mineralogist*, 66, 278–289.
- Yoshii, M., Maeda, K., Kato, T., Watanabe, T., Yui, S., Kato, A., and Nagashima, K. (1973) Kinoshitalite, a new mineral from the Noda-Tamagawa mine, Iwate Prefecture. *Chigaku Kenkyu*, 24, 181–190. (In Japanese)
- Zhang, M., Suddaby, P., Thompson, R.N., and Dungan, M.A. (1993) Barian titanian phlogopite from potassic lavas in northwest China: chemistry, substitutions and paragenesis. *American Mineralogist*, 78, 1056–1065.

MANUSCRIPT RECEIVED SEPTEMBER 24, 2001

MANUSCRIPT ACCEPTED JANUARY 7, 2003

MANUSCRIPT HANDLED BY BRENT OWENS